EUROPEAN ORGANIZATION FOR NUCLEAR RESEARCH

CERN–OPEN-97–023
30 July 1997

THE HIGH-PRECISION X-RAY TOMOGRAPH FOR QUALITY CONTROL OF THE ATLAS MDT MUON SPECTROMETER

D. Drakoulakos, E. Gschwendtner, J.-M. Maugain, F. Rohrbach and Y. Sedykh

Abstract

For the Large Hadron Collider (LHC) of the next millennium, a large general-purpose high-energy physics experiment, the ATLAS project, is being designed by a world-wide collaboration. One of its detectors, the ATLAS muon tracking detector, the MDT project, is on the scale of a very large industrial project: the design, the construction and assembly of twelve hundred large muon drift chambers are aimed at producing an exceptional quality in terms of accuracy, material reliability, assembly, and monitoring. This detector, based on the concept of very high mechanical precision required by the physics goals, will use tomography as a quality control platform. An X-ray tomograph prototype, monitored by a set of interferometers, has been developed at CERN to provide high-quality control of the MDT chambers which will be built in the collaborating institutes of the ATLAS project. First results have been obtained on MDT prototypes showing the validity of the X-ray tomograph approach for mechanical control of the detecting elements at extreme accuracy (below ten-micrometre positioning).

Presented at the 7th Asia Pacific Physics Conference, Beijing, 19–23 August 1997.
(Submitted to Nuclear Instruments and Methods in Physics Research)

1 INTRODUCTION

In the middle of the year 2005, the Large Hadron Collider (LHC) under construction at CERN, will be ready to deliver proton collisions at 14 TeV at luminosities up to 10^{34} cm^{-2} s^{-1}. This is a new energy frontier: it opens a new opportunity for particle physics towards new discoveries in our understanding of matter. However, at the same time, it creates a new challenge for the experiments: very high luminosity, high radiation environment, and very small cross-sections for discoveries lead to unprecedented experimental conditions in terms of the data acquisition rate and signal over background.

After several years of Research and Development, large LHC collaborations are now ready to enter into the construction phase of the huge detectors needed in order to exploit the full potential of the LHC collider for physics search.

1.1 Basic physics motivation

One of the most fundamental questions of the day in particle physics is the origin of the different particle masses. To understand this fundamental question, the Standard Model invokes the existence of a new field, called the Higgs field, and correlatively a new heavy neutral boson, the Higgs (H). Each particle mass, quarks and leptons and the Higgs itself, would then be regarded as the measure of the particle coupling strength to the Higgs field.

The Higgs search is therefore a very important goal for LHC experiments, since the LHC energy reaches the energy range expected for Higgs discovery.

Supersymmetry is currently considered as the strongest competitor for extensions of the Standard Model. SUSY predicts the existence of partners for all known particles quarks–squarks, leptons–sleptons, gluons–gluinos, etc., with masses well suited to the LHC energy range. The Minimal Supersymmetric Standard Model (MSSM) calls for more Higgs states (neutral and charged Higgs). Among many other experimental physics goals, the hunt for SUSY partners will also be a hot challenge for the detectors.

Entering a new energy domain may also lead to unexpected discoveries as has already occurred many times in particle physics experiments. Therefore, the detectors should be ready for all new physics and open to the greatest discovery to be made at LHC: a surprise.

1.2 ATLAS at CERN

One of the two large detectors under preparation is the ATLAS detector ([1], [2]).

ATLAS has been designed as a general-purpose detector for LHC, with efficient and high-resolution tracking, excellent calorimetry and precise muon detection. The inner detector is embedded in a 2 T superconducting solenoid coil placed inside the calorimetry. The calorimeter is installed between the inner tracker and the muon spectrometer which forms the outer shell of the ATLAS detector.

The muon spectrometer surrounding the calorimeter is optimized not only for Higgs search but in order to leave open the possibility to tackle many other kinds of searches in order to exploit the full potential of the LHC. It has been designed as a high-resolution, high-efficiency muon spectrometer with stand-alone triggering and precise momentum-measurement capability over a wide range of transverse momentum, covering with high hermeticity a large

range of pseudorapidity. This was achieved by using an original, well-adapted, magnetic field configuration: large superconducting air-core toroids arranged in an eight-fold symmetry, with a bending power ranging from 2.5 Tm at $\eta = 0$ to 8 Tm at maximum rapidity ($|\eta| = 2.7$).

The detector will fill a huge cavern ($\approx 26 \times 47 \times 30$ m^3) surrounding the collision area at ≈ 90 m under the ground surface.

ATLAS is a very large world-wide collaboration; at present it involves 144 institutions with about 1700 participants. In terms of size, cost, and timescale, this detector will be the biggest ever built for high-energy physics experiments.

2 THE ATLAS MUON SPECTROMETER

The instrumentation of the ATLAS muon spectrometer (see the Technical Design Report [3]), as a sub-detector of ATLAS, has been designed by a collaboration of about 340 physicists from 37 institutes in ten countries, four of them non-Member States of CERN.

High-momentum final-state muons are amongst the most promising and robust signatures for searching for the Higgs. The clearest signal for Higgs production would be through one of the leptonic decay modes of the produced Z bosons ($H \rightarrow ZZ \rightarrow \mu^+ \mu^- \mu^+ \mu^-$), provided the Higgs mass were above ≈ 184 GeV [2m(Z)]. The branching ratio of this decay mode is small ($\approx 0.11\%$) but the signature of this kind of event will be clear and unambiguous.

The performance required for physics in momentum and mass resolutions is at the level of 1%. The transverse-momentum resolution should be constant over the full rapidity range.

2.1 Layout

The spectrometer is shown on Figs. 1–3.

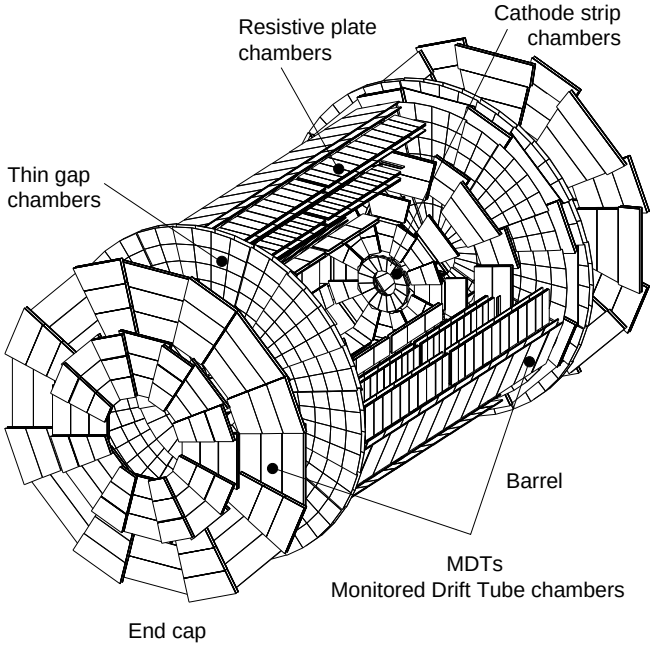

Fig. 1: Three-dimensional sketch of the ATLAS muon spectrometer layout.

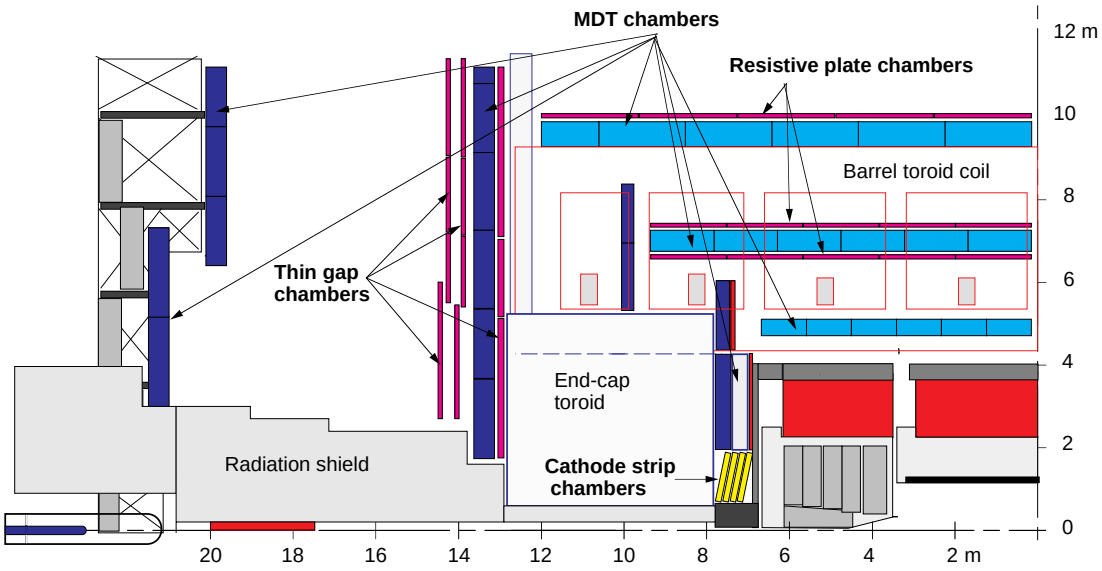

Fig. 2: Side view of the muon spectrometer.

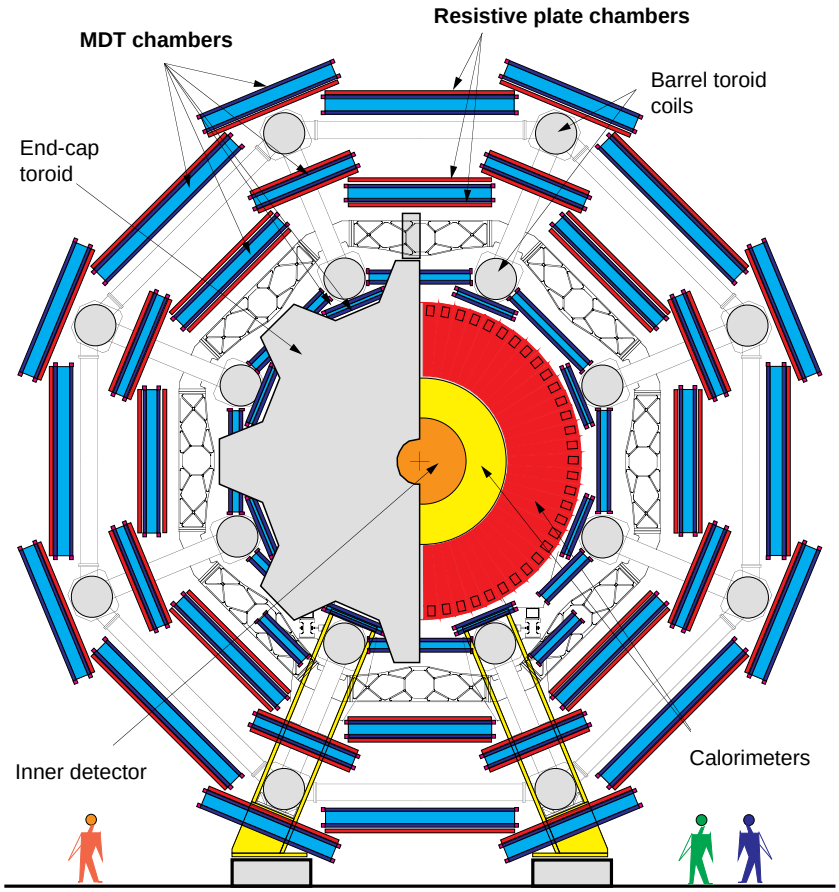

Fig. 3: Cross view of the muon spectrometer.

The design philosophy was to adopt a safe and industrial approach matching all the physics requirements and experimental constraints for getting a reliable, safe, and robust muon spectrometer able to run for at least 10 years without major trouble.

The conceptual layout of the spectrometer is based on a system of three large, superconducting, air-core toroid magnets instrumented with separate-function trigger and high-precision tracking chambers. This magnet configuration provides a field that is mostly orthogonal to the muon trajectories, producing a maximum bending power, which is needed for momentum resolution and charge-sign determination at the highest energies, while minimizing the degradation of resolution due to multiple scattering.

Last but not least, another important consideration is to produce an economical design that allows a total surface of about 5000 m^2 to be covered at an affordable cost.

2.2 Momentum measurement

Over most of the pseudorapidity range, a precision measurement[1)] of the track coordinates in the principal bending direction of the magnetic field is provided by Monitored Drift Tubes (MDTs) and Cathode Strip Chambers (CSCs). The MDT chambers are arranged in three layers all around the calorimeter in order to determine the momentum with the best possible resolution. The CSCs are used for the very forward area where the particle flux is too high for the drift chambers.

With this layout, a three-point measurement is available (see Fig. 4) by installing three stations of multilayer monitored drift chambers covering the full rapidity gap with high hermeticity. The drift MDT chambers are called ‘monitored’ because a continuous monitoring of the internal chamber deformations is done. In addition to this on-line survey, the position in space of each chamber is also monitored with the required precision (≤ 20 μm).

With this layout, the momentum resolution, as can be seen on Fig. 5, is typically 2–3% at 100 GeV/*c* over most of the kinematic range.

The muon spectrometer is designed for a momentum resolution $\Delta p_T/p_T < 1 \times 10^{-4}\, p_T$, where p_T is in GeV, for $p_T > 300$ GeV. To achieve this resolution by a three-point measurement, with the size and bending power of the ATLAS toroids, each point must be measured with an accuracy of about 50 μm. This sets the scale for the requirements on the intrinsic resolution, the mechanical precision, and the survey accuracy of the muon chambers.

The momentum resolution of the spectrometer is limited by the intrinsic detector resolution, MDT calibration errors, chamber positioning uncertainties, multiple scattering, and statistical fluctuations of energy loss. At smaller momenta, the resolution is limited by multiple scattering to a few per cent, at higher momenta it is dominated by chamber precision and alignment (Figs. 6 and 7).

---

1) Charged particles, with 300 GeV/*c* momentum, crossing the toroid magnets of the muon spectrometer, will have very large radius of curvature producing small sagitta signals ($s \approx 1.5 \div 5$ mm) over the long muon trajectories ($5 \div 15$ m) between the three measuring stations. In order to achieve the required precision in the momentum measurement, the sagitta must be determined with a precision of $15 \div 50$ μm.

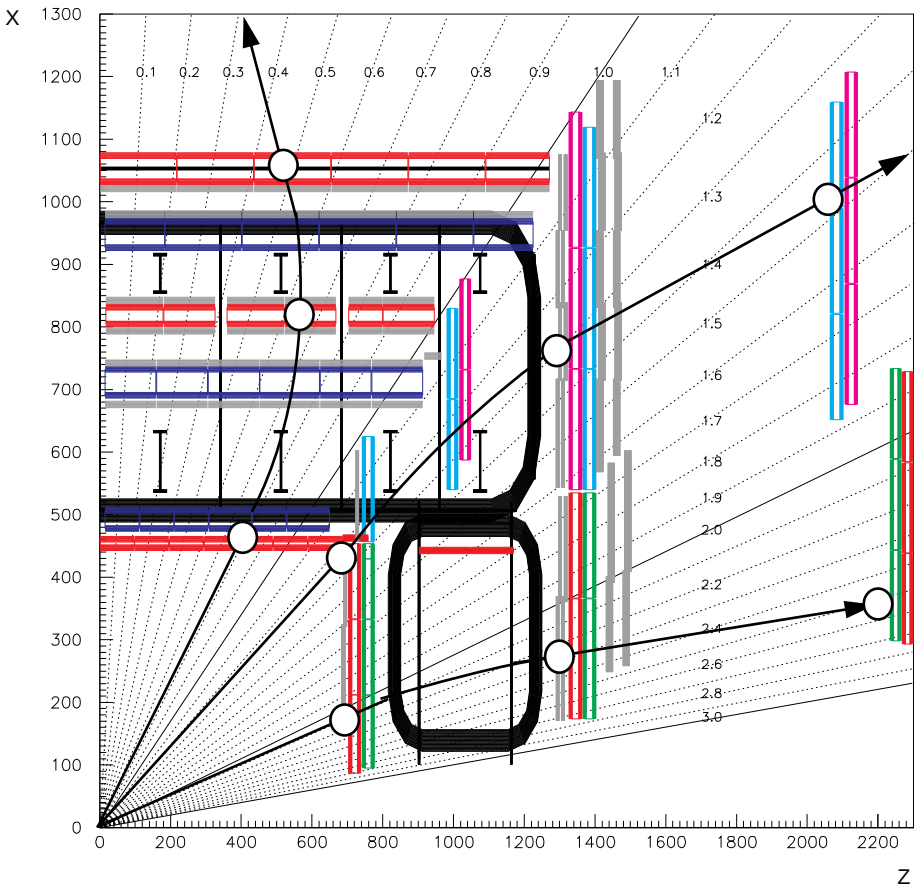

Fig. 4: Longitudinal cross-section in the bending plane of the spectrometer showing the barrel and end-cap magnet air-coil toroid configuration. It shows the pseudo-rapidity coverage of the muon spectrometer from 0 to 2.8 and a sketch of the layout principle of the three detecting muon stations.

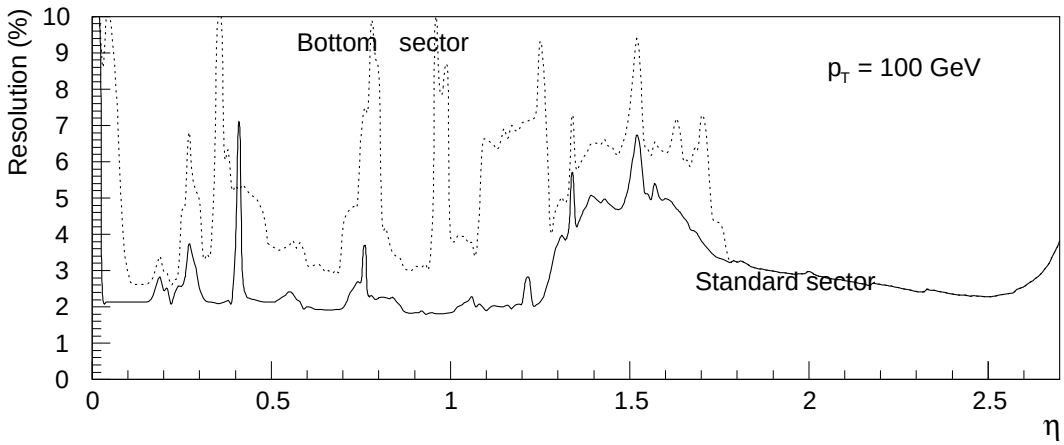

Fig. 5: Momentum resolution for p_T = 100 GeV averaged over all azimuthal angles.

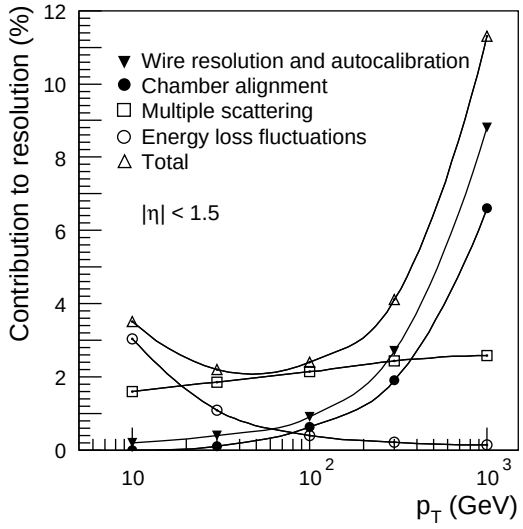

Fig. 6: Contributions to the momentum resolution in the muon spectrometer, averaged over $|\eta| < 1.5$.

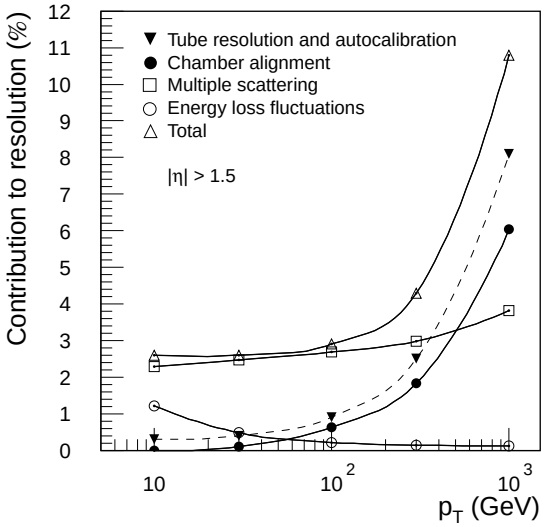

Fig. 7: As Fig. 6, for $|\eta| > 1.5$.

2.3 The MDT chambers

The task in numbers is impressive: the total number of MDTs is 1194 making a total area of 5500 m^2. The total number of readout channels (number of drift tubes) is 371 488 and the total length of the tubes ≈ 1141 km.

2.3.1 The drift tubes

The basic detection elements of the MDT chambers are drift chambers made of aluminium tubes, of 30 mm diameter and 400 μm wall thickness, with a 50 μm diameter central W–Re wire. The tubes are operated with a non-flammable Ar-CH_4-N_2 mixture at 3 bar absolute pressure.

The tubes are produced by extrusion from a hard aluminium alloy, and are available commercially. They are closed by endplugs which provide for accurate positioning of the anode wires, wire tension, gas tightness, and electrical and gas connections. The drift tubes can be manufactured to tight mechanical tolerances which are well-matched to their intrinsic resolution properties, mostly using automated assembly procedures. The tube lengths vary from 70 cm to 630 cm.

The envisaged working point provides, for a good linear space–time relation with a maximum drift time of ~ 500 ns, a small Lorentz angle and good ageing properties due to small gas amplification. Using the time–drift distance relationship, the single-wire resolution is typically 80 μm when operated at high gas pressure (3 bar).

2.3.2 Chamber design

The muon chamber layout was optimized to reduce the number of different chamber sizes:

– The barrel chambers are of rectangular shape with sizes from 2 to 10 m^2.
– The end-cap chambers are of trapezoidal shape. Their sizes range from 1 to 10 m^2 for individual chamber modules and up to 30 m^2 when several of them are preassembled for installation.

The chamber design must guarantee reliability and stability of construction and operation for the anticipated lifetime of the experiment in an irradiated environment. The basic design is shown on Fig. 8.

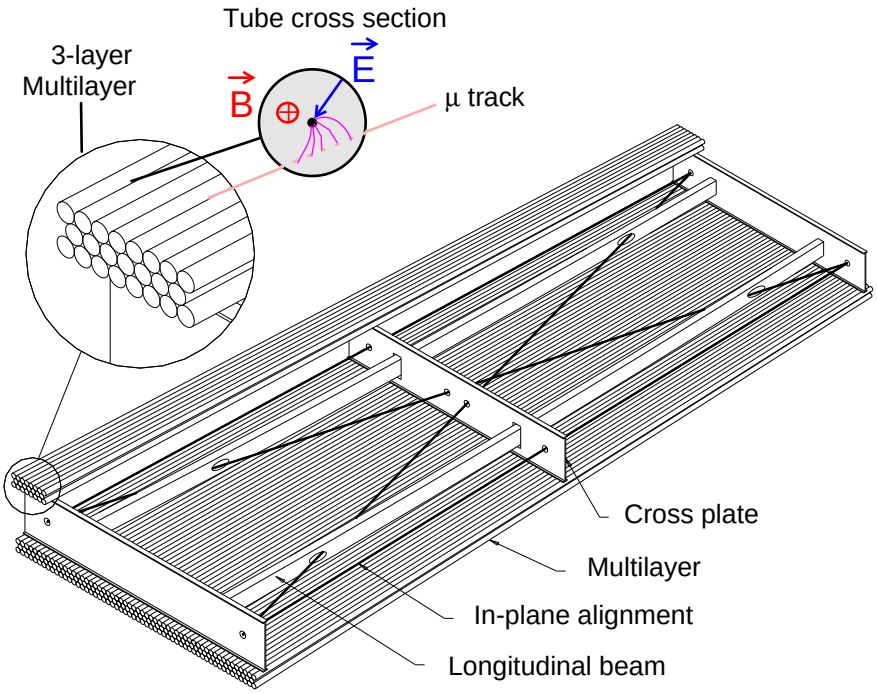

Fig. 8: Schematic drawing of a rectangular MDT chamber constructed from multilayers of three monolayers each, for installation in the barrel spectrometer. The chambers for the end-cap are of trapezoidal shape, but are of similar design otherwise. In the toroidal magnetic field, the tubes are oriented essentially parallel to the field lines.

To improve the resolution of a chamber beyond the single-wire limit and to achieve adequate redundancy for pattern recognition, the MDT chambers are constructed from 2×4 monolayers of drift tubes for the inner, and 2×3 monolayers for the middle and outer stations. The tubes are arranged in multilayers of three or four monolayers, respectively, on either side of a rigid support structure. The support structures, the 'spacer frames', provide for accurate positioning of the two multilayers with respect to each other, and for mechanical integrity under effects of temperature and gravity. As an example of difficulties encountered when seeking to reach the required resolution, the drift tubes which are not mounted vertically are bent slightly in order to match their shape to the gravitational sag of the wires.

The structural components of the spacer frames are three 'cross-plates', to which the drift tube multilayers are attached, and two 'long beams' connecting the cross-plates. The frames need to be constructed to a moderate mechanical accuracy of ± 0.5 mm only; accurate positioning of the drift tubes is provided by the assembly procedure. The chambers will be attached to the rail structures of the spectrometer by three-point kinematic supports. Once a chamber is installed in its final location in the spectrometer, mechanical deformations are monitored by an in-plane optical system; hence the name 'Monitored Drift Tube' chambers. The spacer frames support most of the components of the alignment system.

MDT chambers are made for robust and reliable operation. This is achieved thanks to the mechanical concept which provides a solid separation of detecting cells and a good electrical shielding of neighbouring wires.

Chambers must withstand very long storage time followed by very long running periods. In order to reach the required momentum resolution, all MDT chambers must be constructed with 20 μm mechanical accuracy.

2.4 Quality assurance for MDTs

The MDT project in ATLAS is on the scale of a very large industrial project aiming at an exceptional quality of construction in terms of accuracy (≤ 20 μm), material reliability, delivery and assembly schedule. The only known engineering way to reach this ambitious goal is to establish quality management and quality systems, inspired by the 9000 ISO standard ([4] –[8]), adapted to the ATLAS project from design to final assembly. In particular, taking into account the large size and complexity of the project, the implementation of a Quality Assurance Plan (QAP) [9], [10] is needed to reduce cost and improve quality.

The X-tomograph quality control platform may be considered as one of the key instruments needed for the MDT QAP.

The production of the Monitored Drift Tube chambers is based on the concept of very high mechanical precision and the use of X-ray tomography as a quality control platform for the mechanically achieved precision.

The successful completion of the project will depend, in the first place, on the timely construction of the MDTs. After the completion of prototyping, which should occur by the beginning of 1998, each assembly site will construct a so-called 'module zero' of each type of chamber that it will later fabricate in series, in order to certify the assembly process and gain experience for the series production. These 'module zeros' will be measured and qualified at CERN. This feed-back control procedure is a part of the quality insurance plan. Series

production of most chambers will take place from 1999 until 2003 and delivery to CERN will have to be organized in order to match smoothly both the production schedule and the quality control platform availability.

The chambers will be delivered to CERN equipped with readout boards, which will allow for easy installation of the front-end electronics. As will be shown later in this paper (see Section 3.2.2), it would be possible to join the electrical and mechanical control of the wire positioning of each drift tube using the 'active method' procedure for X-ray scanning.

3 X-RAY TOMOGRAPHY

The development design, construction, and tuning of an X-ray tomograph suited for the MDT quality control was the aim of the X-ray Quality Control 'X-QC' project.

3.1 Basic principle

The choice of X-ray tomography as a quality control tool for the MDT project was based on two essential features:

1) The ability of X-rays to detect micron-sized tungsten wires hidden inside the aluminium drift tubes of the muon detector. Sharp absorption spikes are observed either as a shadow seen by a X-ray detector placed under the chamber (passive method) or as a detection peak registered by the muon tube wire itself hit by X-rays (active method, see Section 3.2.2).
2) The possibility to produce narrow collimated X-ray beams allowing to reach detection profiles with the required peak position detection accuracy (1 to 2 μm).

The value of the absorption coefficient for X-ray photons is very sensitive to attenuating materials and to the X-ray energy. If δ is the density, Z the atomic number of the material and W the energy of X-rays, the mass absorption coefficient μ/δ varies as $\approx (Z/W)^3$ at 40 keV. The large difference in the attenuation coefficient values between tungsten and aluminium materials is used to detect signal wires in the multilayer structure of the MDTs. At lower energy the absorption becomes too high and at higher energies the Z effect becomes too small for a good detection. The optimum energy range for this application is between 30 and 50 keV.

3.2 Basic procedure

A narrow X-ray beam is precisely moved across a section of the MDT chamber. A scintillator, installed under the chamber, records the absorption profile during a scanning along the multilayer cross-section of the chamber. The data are analysed and provide projective measurement. Stereo-measurements are possible, when using different inclination angles of the X-ray beam. From the data registered, a two-dimensional map of wire positions can be reconstructed. Every chamber is scanned in a few positions along the tube length. A full calibration of the muon chambers produces a list of all the wire coordinates in two dimensions. Using an external fiducial wire installed along the chambers, a 3-D map can finally be constructed.

After the analysis of raw data, the results are stored in a database providing the full list of the wire position and accuracy.

We can measure the MDT chamber's wire position using two different methods.

3.2.1 The 'passive' method

This procedure may be seen as the conventional method for many X-ray applications which exploits the significant X-ray absorption contrast between different materials. It is based directly on the good transparency of a MDT chamber to X-rays and on the strong absorption difference of X-rays at 40 keV between the aluminium material of the 400 μm wall thickness of the tubes (≈ 12%), the 3 bar gas in the tube (≈ 0.6%), and the 50 μm tungsten anode wires (≈ 65%). The output intensity of the X-ray beam is measured by a scintillator. Figure 9 shows the counting rate of the scintillator versus the X coordinate[2)] measured when scanning a small four-layer chamber prototype.

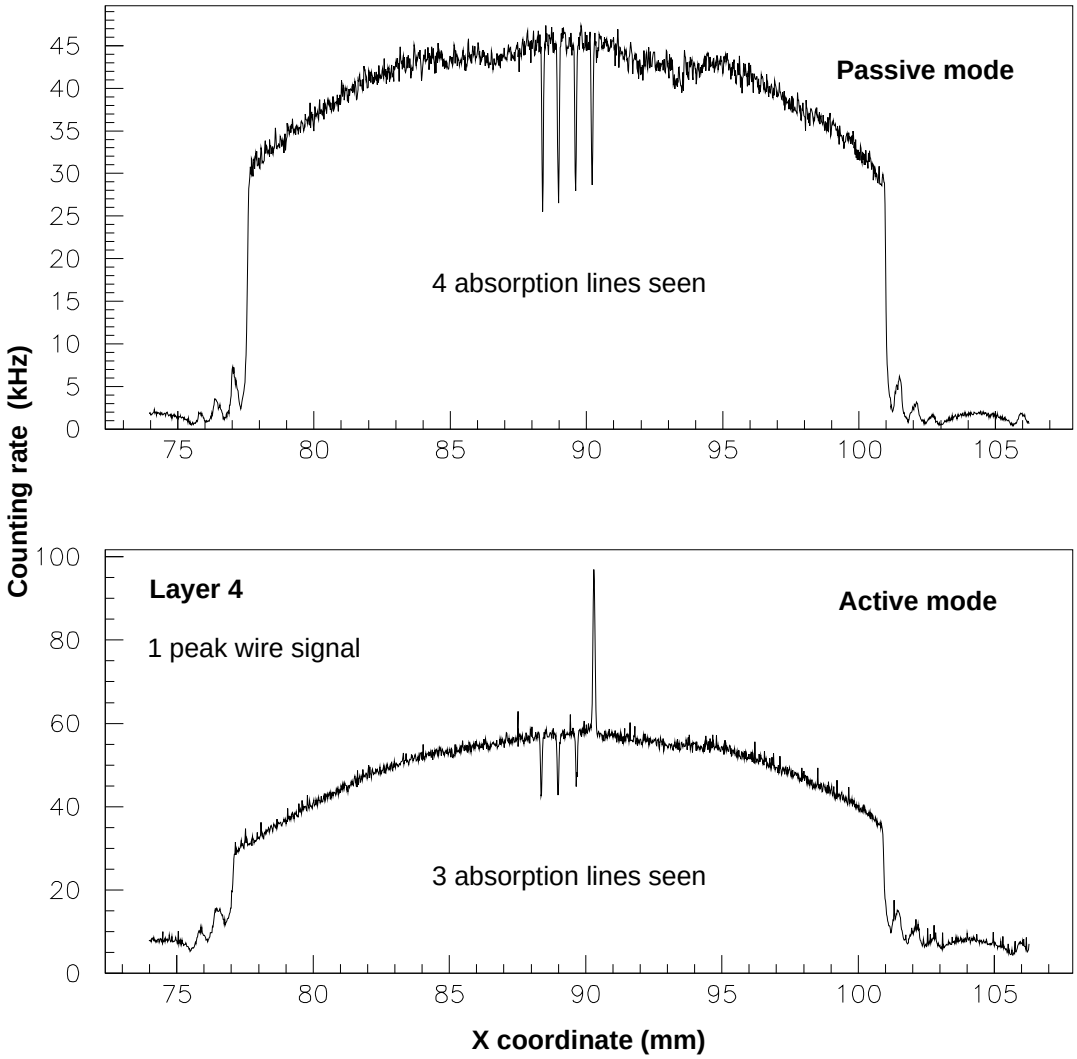

Fig. 9: Passive and active scanning methods of a small four-layer chamber prototype.

2) In this paper, we exclusively use the natural X-ray tomograph coordinate system (see Ref. [10]), X (scanning direction, in the horizontal plane), Y (in the horizontal plane, perpendicular to the scanning direction) and Z (the vertical coordinate). MDT uses another system of coordinates: x (along the tubes), y (normal to chamber plane) and z (across the tubes). Consequently the correspondence is as follows: X → z, Y → x, Z → y.

3.2.2 The 'active' method

This second procedure is based on the position-dependence efficiency of drift tubes for X-rays. When the X-ray beam hits the wire, photoelectrons, Auger electrons and fluorescence are produced at a much higher rate than in the gas or in the walls. These radiations have a high probability of escaping from the surface of the wire and of being detected by direct ionization in the gas. Figure 9 shows the wire signal from a tube belonging to the bottom layer of the small chamber prototype. The three wires in the upper layers above the active tube are clearly seen as absorption peaks by the active tube: they produce a shadow effect which is observed as inverted peaks compared to the tube wire signal itself.

The relative intensity of the signals is not only proportional to the absorption power of the material but also to the probability of photoelectrons to escape from the material and to ionize the detecting gas of the drift tube.

3.2.3 Detection of the tube wall

The aluminium tube walls can also be seen in the same way, provided the X-ray beam flux is constant during the scanning of the tube cross-section. At a given X-ray energy, the expected signal from the wall should be about half of the one obtained from the wire:

$$\text{signal ratio} \approx \frac{\left(\frac{\mu}{\delta}\right)\sqrt{r\delta}\Big|_{AL}}{\left(\frac{\mu}{\delta}\right)\sqrt{r\delta}\Big|_{W}}$$

where: (μ/δ), δ, r are respectively the mass absorption coefficient for X-rays in the material, the density, and the radius of the aluminium tube and of the wire.

In order to measure the centring of the wires inside the tubes, it is necessary to keep the intensity of the photon flux stable during the scanning of each tube. This cannot be done using a fixed-angle scanning because of the masking effect of the other aligned tube walls of the multilayers. In the active mode, however, using a rotating X-ray beam moved step by step across the chamber according to the pitch and rotating the beam at each step from wall to wall, the centring of the wires could be precisely ($\leq \approx 20\ \mu m$) determined for each tube using a microprecision industrial rotator.

3.3 Full quality control for MDTs

As we have seen, the active method requires having the drift chamber in a working state. It would then be possible to combine and integrate in a single run the mechanical and electrical control of all the detecting channels. Moreover, should the tomograph be equipped with rotating heads, the control of the centring of the wires in all tubes could be done at the same time in an automatic way.

4 THE PIONEER WORK

The first manual and then automatic X-ray scanning of drift tubes was done in JINR, Dubna during the years 1988–90 [11]. Nice shadow signals from the W and Cu-Be wires were detected through up to 11 mm of aluminium material.

In 1992–94, the joint CERN–JINR team constructed a high-precision X-ray scanning prototype, with 600 mm scanning length (5 μm accuracy) using a 1 kW power X-ray tube [12].

In 1995, at CERN, a MDT muon chamber prototype with 2×4 layers of tubes was scanned with a single X-ray beam providing projective measurements with the expected precision [13]. The 600 mm scanner prototype was upgraded in 1995–96 to test the possibility of achieving stereomeasurements.

4.1 The small X-ray tomograph

The measurement of the position of the wires in two dimensions, along a cross-section of a chamber, was performed by using a 600 mm microprecision linear stage and two successive measurements obtained from two different X-ray beams with opposite and fixed inclination angles installed on the same cart.

4.1.1 Scanning angle

The selection of the two inclination angles, Θ_1, Θ_2, the so-called 'scanning angle' relative to the perpendicular to the chamber plane, was an important issue under consideration [14] for two reasons:

- They define the stereo angle ($|\Theta_1| + |\Theta_2|$) and consequently the two-dimensional accuracy of the position of the wires.
- The absorption peak pattern of the wires, within a corridor defined by the Θ angle, must show well-separated absorption signals. This pattern is very sensitive to the Θ angle and depends upon the chamber structure characteristics, i.e. the height of the spacer, the symmetry between the two multilayers, and the horizontal and vertical wire pitch.

The most convenient choice is to align the beams in the natural $\pm 30°$ corridors of the multilayers. The angle must be chosen a little bit higher in order to tune the wire signal gap separation.

4.1.2 Scanning method

The precision of the measurement relied entirely on the quality of the mechanics of the industrial linear scanner. All systematic corrections were based on the calibration curves delivered by the constructor.

To first order, the geometric reconstruction requires the knowledge of only three mechanical parameters: the linear scanning position, the vertical straightness, and the angular displacement around the axis perpendicular to the scanning cross-section plane (pitch angle). The excellent repeatability (better than 1 μm) of the linear stage was crucial for achieving high reconstruction accuracy. The pitch was monitored using a high-precision tiltmeter.

The relation between the X position and the Θ angle of each beam shows that the main error in the determination of the position of the wires depends upon the accuracy of the

determination of the absolute value of the two scanning angles. A calibration procedure using a precise triangle tooling was developed in order to determine the scanning angles within the required accuracy (below 7 μrad in order to reach the 10 μm space accuracy).

4.1.3 Main result

The small 600 mm scanner demonstrated the validity of the fixed stereo-angle scanning approach and the two-dimensional measuring power accuracy of both methods (passive and active) with an excellent result on the local accuracy of the reconstruction;

– 6 μm r.m.s. was obtained [14], when measuring a small chamber prototype (4×8 tubes).

It showed the importance of the corrections based on the *Q* angle monitoring and on the availability of reproducible calibration plots for the high-precision small linear stage [15].

5 THE LARGE X-RAY TOMOGRAPH

5.1 The challenge

The maximum width of the standardized MDT chambers has been fixed at 2160 mm. Therefore, the scanning span of the tomograph has been frozen to be 2200 mm. Owing to the novelty of the micron-sized X-ray beam technological approach, scaling the small tomograph prototype from 600 mm to 2200 mm without reducing final accuracy was not a simple task.

The main challenge was to provide in short time to the constructors, reliable results on the wire positioning of different chamber prototypes built with 20 μm accuracy specification. The large X-ray tomograph prototype had consequently to achieve a better accuracy, aiming at 10 μm, and be built within stringent time and money constraints.

5.2 Design considerations

It was decided to keep the same approach as for the small tomograph, but to add a full monitoring of the movement of the cart supporting the two X-ray beams during the scanning. It was indeed outside of our budget and time availability to build a precise and repeatable mechanical system with a few microns accuracy over such large distances. Consequently, we chose for the main structure of the tomograph, standard high-precision mechanics combined with ultimate precision survey tools in order to monitor the main parameters controlling the X-ray beam position in space during the scanning. In this respect, industrial laser interferometers were used for monitoring Z (the vertical straightness), X (the horizontal displacement) and $\Delta\Theta$ (the pitch angle variation).

For the construction of the other parts and for the software of the tomograph, reliable industrial choices were made whenever possible.

5.3 Prototype specifications

The main specifications for the large X-tomograph were as follows:

1) The accuracy must reach a value below 10 μm in X and Z, over the full cross-section of the measured chambers in order to fit the expected accuracy of the chamber construction (20 μm r.m.s.) in view of a full, safe, and secure quality control.
2) The prototype should accommodate for the biggest chamber size (max. 2200 mm in X, 6000 mm in Y, and 600 mm in Z).
3) The prototype should provide automatic measurements on all chamber cross-sections.
4) Without taking into account time overheads, chamber installation, and thermal stabilization, the prototype should make possible the measurements of chambers at a rate of one chamber per day.
5) The prototype, at least at a later stage, should give the possibility to measure the centring of the wires in all tubes.

The long-term goal of the X-QC project is to prepare a platform for measuring all MDTs, if technically possible within the constraints.

5.4 Construction

Figures 10 and 11 show the large X-tomograph prototype designed and built at CERN during 1996. Owing to the necessity of a very stable environment, the tomograph was installed in a clean room in building 188 ground floor (one of the most stable ground floors at CERN) with temperature control $T \leq \pm 1°C$.

At the early stage, the basic design concept for the construction of the first prototype could not follow all the specifications previously quoted, but only the first two criteria could be considered [points 1) and 2) in Section 5.3].

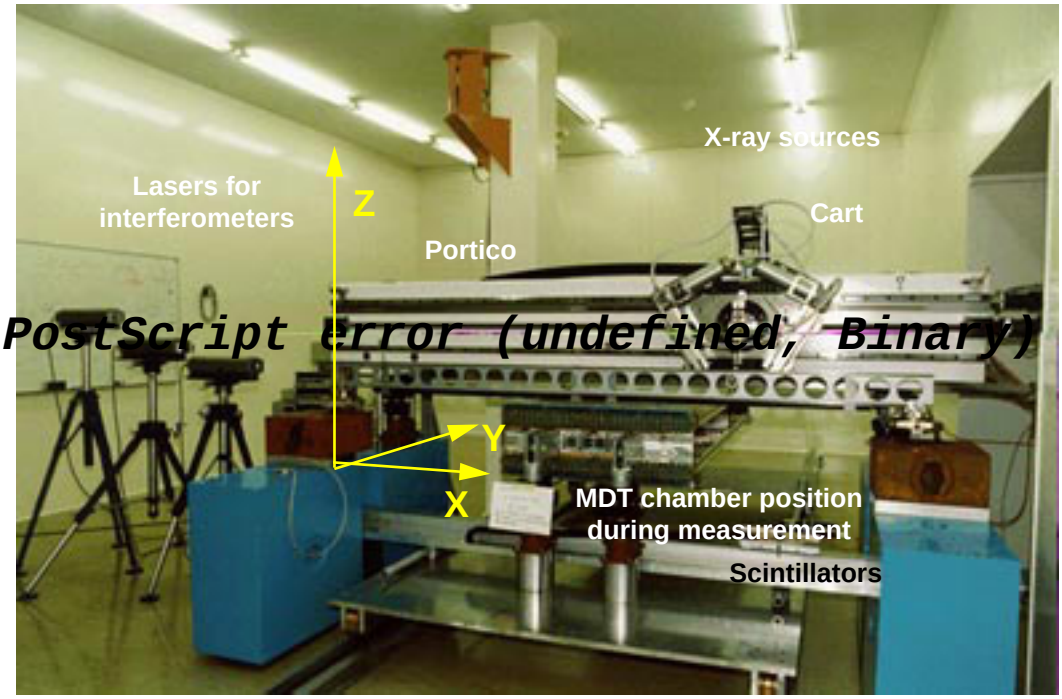

Fig. 10: The X-ray tomograph prototype. The natural reference system for the tomograph is indicated.

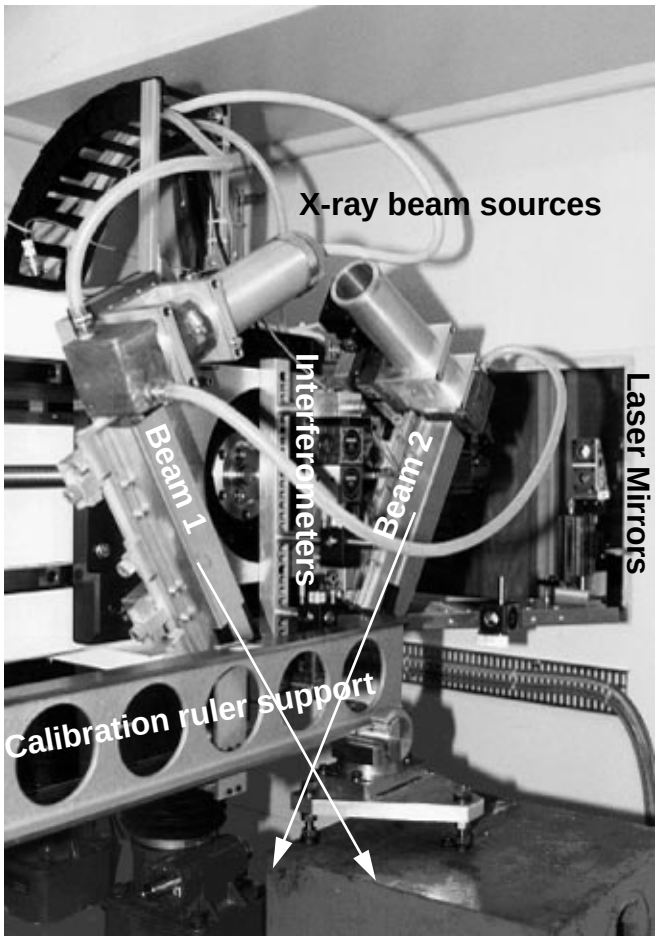

Fig. 11: The rolling cart with the two X-ray sources and the three interferometers for monitoring X, Z and Θ.

The large tomograph prototype consists of:

1) A fixed 3500 mm iron portico equipped with a precise motorized cart rolling along the X axis.
2) The rolling cart is equipped with two collimated X-ray beams at $\approx \pm 30°$ with respect to the Z axis. The $\approx 60°$ stereo angle has been chosen on the basis of our previous experience and fits perfectly the tube corridors, provided the spacers between the multilayers are correctly chosen. The X-ray beams have a cross-section of about 30 μm $\times$ 8 mm and a divergence of about 60 μrad, the longer axis being aligned along the wires to be measured.
3) A computer control of the X displacement which provides steps as low as 10 μm.
4) Three interferometers[3)] which monitor the main parameters of the scanner movement: the linear X value, the pitch angle (rotation around the Y axis), and the vertical straightness. The yaw (rotation around the Z axis) and the horizontal straightness are not monitored as they would have only a second-order effect in the corrections. The interferometers allow a monitoring with an accuracy of 1 μm for linear, 1 mrad for angular parameters over the full range of the scanner.

---

3) At the early stage, the interferometers were not fixed to the tomograph. They were used for testing the validity of the interferometer monitoring concept.

5) A tilt-meter for measuring the roll angle (rotation around the X axis).
6) A calibration ruler split into two parts and placed above the chamber to be measured. It consists of two precisely (1 μm r.m.s.) optically measured patterns of wires mounted on a carbon fibre support. This ruler provides two layers of reference wires giving two very precise peaks which appear in the shadow pattern every 30 mm as seen on Figs. 12 and 13. This calibration ruler is used to check the stability and reliability of the X-tomograph and to provide a calibrated grid frame for the two-dimensional stereo reconstruction.
7) A manual rolling cart to support and align the chamber to be measured. It moves under the portico, along the Y axis, over 12 m to accommodate the longest BOL MDT chambers. It can position the chamber under the portico with an accuracy of 1 mm in Y.
8) One small moving cart enslaved to the X-ray cart, supporting two scintillators, optimized for the X-ray beam energy spectrum, following the beams in order to record the two stereo shadowgrams simultaneously.
9) The control of the tomograph movement, the data-acquisition and parameters monitoring are supported by an online program written in LabView language working on PC [16].
10) Two X-ray high-voltage power supplies (up to 60 kV, 20 mA). The two high-voltage cables feeding the X-ray tubes move in synchronism with the scanner on a separate cart in order to ensure a perfect stability of the X-ray rolling cart.

The large X-tomograph prototype — called DiMiTriX — was made operational at CERN on 11 November 1996.

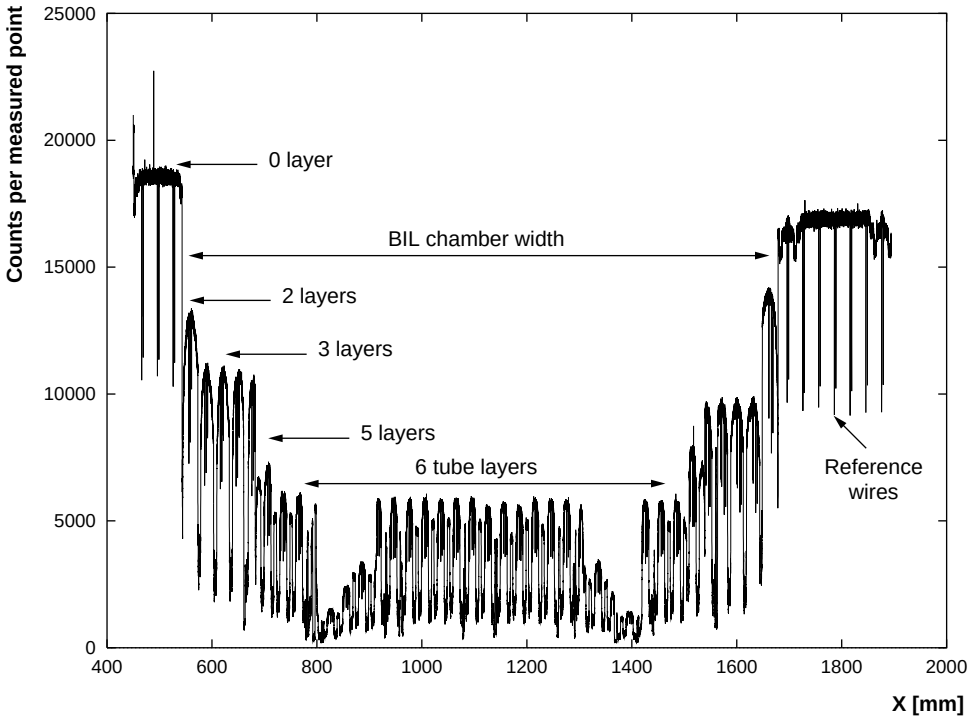

Fig. 12: Shadowgram[4)] of the BIL-I prototype chamber. The regions of increased absorption between 800 mm and 1000 mm, or 1300 mm and 1500 mm are due to the chamber Al frame. The absorption of the layers is seen and the number of counts per measured point remains large enough for a good statistical significance even for the deepest layer.

4) Scanning parameters: average speed per measured point including data taking overhead: 48 μm per second. Total scan: 1450 mm, 8:26 hours, one data point every 20 μm X displacement, 40 ms per point for counts.

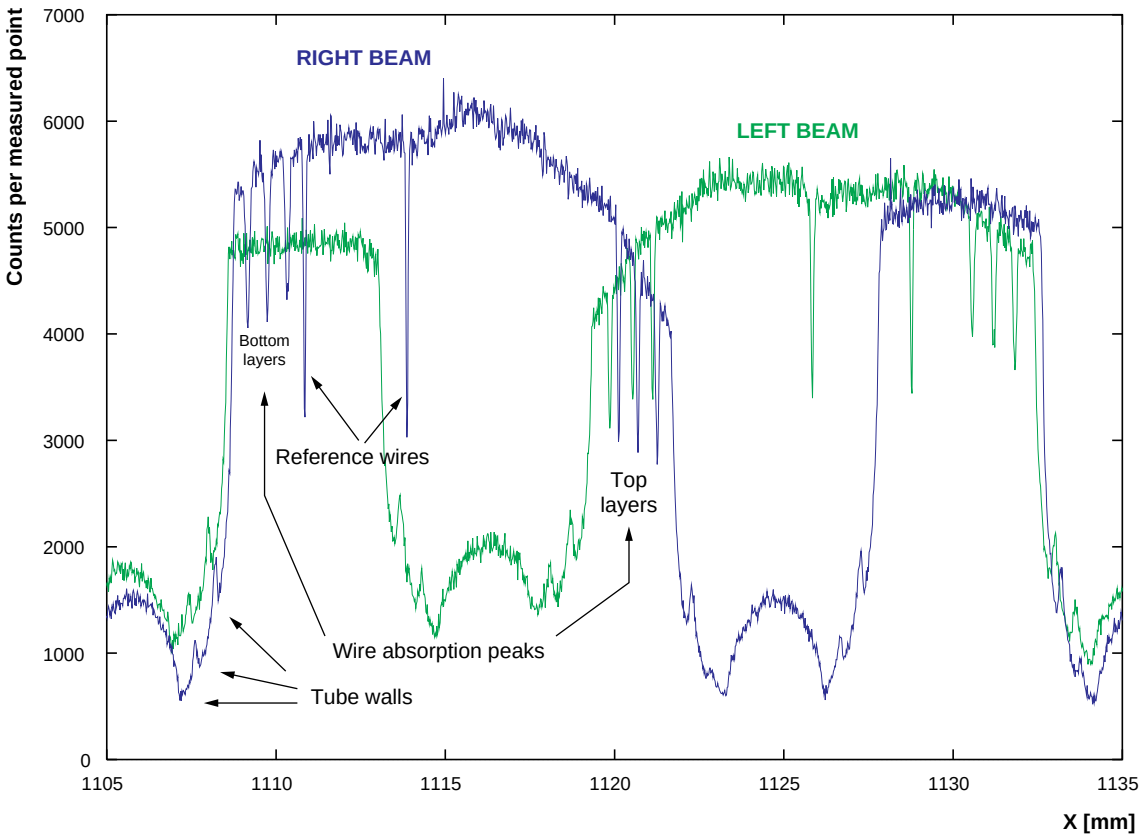

Fig. 13: Shadowgram (zooming from Fig. 12) of a BIL-I chamber prototype obtained for the left and right beams during a same scanning. The shadowgram covers one full corridor of the chamber. Wires, walls, and reference signals are indicated.

5.5 Muon chamber prototypes measurements

Four prototypes of different MDT chambers, delivered by the institutes to CERN, were checked during the first measurement campaign (November 1996 to March 1997).

Each of the four chamber prototypes[5)] was measured at least in four cross-sections along the tube length. In order to start more investigations, different scans were done with tubes under pressure (CO_2, 3 bar), high voltage on the wires, and using different X-ray energies. Preliminary results have been obtained in the one- and two-dimensional analyses for the four prototypes. A typical shadowgram can be seen on Fig. 12 and a zoom pattern on Fig. 13. With the present data acquisition system, the scanning time for a one-metre scan is about six hours (with one point measured every 20 μm along X).

Consequently, the total time for checking one MDT chamber is of the order of one week. It will be one of the major tasks of the next upgrade to reduce the scanning time.

---

5) The Roma–Pavia–Seattle BIL prototype, the Frascati–Cosenza BML prototype, the Protvino BIL prototype, and the MPI/Munich BMS prototype. They will be respectively referred to in this paper as the BIL-I, BML, BIL-R and BMS chamber prototypes.

5.5.1 One-dimensional analysis and results

The absorption spectra of the two X-ray beams are provided as a plot of counting rate versus the X position given by the linear interferometer. Each scan delivers a file of about 12 Mbyte of raw data which consists of a list of interferometer parameter values and counts registered over 40 ms at each 20 μm step. Storage and back-up protection of the raw data are under study (development of high-compression algorithms).

The main steps of the one-dimensional analysis are:

1) The pattern recognition of the left and right X-ray projective shadowgrams. This is achieved by comparing the absorption peak pattern to the expected one (obtained by simulation).
2) After identifying the peaks in each absorption spectrum, one fits the following Gaussian polynomial function:

$$f(X) = p_0 + p_1 X + c_1 \times \exp - (X - pos)^2/2\sigma^2$$

where:

- X is the coordinate measured by the linear interferometer,
- pos is the wire position,
- p_0, p_1, c_1, pos and σ are free parameters,
- the function $f(X)$ was fitted to a $\pm(100 \div 200)$ μm region around each peak [$(20 \div 30)$ points per profile].

Table 1 shows the results obtained for the four prototypes.

Table 1: Results of the pitch value from 1-D analysis for the four chamber prototypes measured. The values are in micrometres (pitch values = 30 000 + table numbers), they are the average results of the two X-ray beam scans; the r.m.s. values are shown in parentheses. For the BMS chamber, the results are taken from a single module of the chamber multilayer (the BMS prototype was made of four different modules per multilayer).

		BIL-I		BML		BIL-R		BMS	
		Beam 1	**Beam 2**	**Beam 1**	**Beam 2**	**Beam 1**	**Beam 2**	**Beam 1**	**Beam 2**
Nominal Pitch		8		45		100		100	
Multilayer 2	**Layer 4**	-	-	-	-	-	-	103.3	
								(18.1)	(28.6)
	Layer 3	7.7		47.05		100.0		101.8	
		(15.4)	(17.6)	(17.0)	(16.7)	(37.0)	(28.0)	(30.9)	(26.1)
	Layer 2	6.9		46.9		99.95		100.95	
		(22.5)	(25.4)	(17.8)	(13.4)	(23.1)	(25.9)	(24.7)	(19.3)
	Layer 1	6.55		47.15		99.65		99.05	
		(19.3)	(16.5)	(14.1)	(13.1)	(26.3)	(19.0)	(17.7)	(19.9)
Multilayer 1	**Layer 4**	-	-	-	-	-	-	99.85	
								(25.5)	(23.2)
	Layer 3	7.0		47.0		99.85		99.85	
		(16.3)	(21.1)	(25.2)	(24.4)	(10.2)	(16.7)	(25.8)	(20.6)
	Layer 2	7.85		46.55		99.25		95.9	
		(14.7)	(17.6)	(22.8)	(22.5)	(15.7)	(18.5)	(23.4)	(25.6)
	Layer 1	7.6		46.75		99.15		92.7	
		(16.1)	(15.0)	(23.9)	(26.5)	(13.8)	(15.5)	(20.7)	(25.3)

Each layer is fitted to a grid function (LayerShift + i × LayerPitch) in order to find the best estimate of the layer parameters and their r.m.s. This is only valid locally in X, as no more corrections due to the other scanner parameters are possible in the one-dimensional analysis.

Although the plane of the chamber is usually tilted with respect to the scanning X axis (alignment), the mean values of the pitch distance are meaningful: the two values obtained from the pattern analysis produced by the two beams can be averaged in order to get a very good approximation of the distance between wires (the error induced by this approximation is only ≈ 0.3 μm for a tilt below 5 mrad).

The precision of the tomograph, for the determination of the projected position of a wire along the X axis, has been established by minimizing the distance between the measured position and the calibrated values found for the reference wires of the calibration ruler: it leads to a value of 13 μm. The results have been calculated without taking into account individual features of chambers (different lengths of tubes in one chamber, technological shifts between layers etc.) which may significantly change the values. It is necessary to take care when comparing the results for different chambers.

Quite a few interesting comments and conclusions can be made:

- For the BIL-I prototype, all scans and all layers give an average pitch of 30 mm + 7.3 μm with a standard deviation 0.5 μm in agreement with the nominal design parameter (8 μm). The r.m.s. of the pitch is within the 20 μm r.m.s. construction design requirement for upper and lower layers. However, for the intermediate layers of the multilayers, the r.m.s. is worse.
- For the BML prototype, the r.m.s. of the pitch in the central cross-section is quite good (below 20 μm) but bigger than 20 μm (up to 40 μm for some layers) at both chamber ends.

It is striking and encouraging to point out that these results have already been of great interest to the prototype chamber constructors and will help in the final decision for the technological and assembly issues and choices. A more detailed report is in preparation [17].

5.5.2 Two-dimensional analysis and results

A program, known as ‘scana’, has been developed and written for the two-dimensional analysis of the raw data produced by the two X-ray beams of the tomograph. It should be, as a final goal, fully automatic, delivering the results shortly after the measurements.

The organization of the ‘scana’ program for the 2-D analysis consists of four main parts:

1) Automatic pattern recognition of peaks and layers, and matching of tube wires and calibration wires for the two beams.
2) Calculation of the position of the peaks similar to the one dimensional case. Determination of the geometrical parameters of the scanner using the precise calibration rulers and the interferometer measurements.
3) Chamber wire position analysis which provides the X, Z position of all detected wires. Calculation of the displacement of the wires with respect to an ideal template fit with five parameters fixing the position of the chamber in space. Determination of some integral parameters with a view to studying the possibility to establish integral chamber quality factors.

4) Graphical presentation of results, Web publishing and saving. Listings of all analysed data, giving the position of all detected wires together with preliminary analysis of the results. All tables and maps are provided on the Web [18].

As a consequence of the use of all possible corrections, made possible thanks to the interferometer control, the analysis gives interesting, good, and coherent results: the residuals are around 6 μm for the calibration ruler. Consequently, the positioning accuracy over the whole domain of the measurements in X and Z is below or equal to 10 μm.

At present, the program has been producing preliminary results for the four prototype chambers. In Table 2 we show, as an example, the results for the two BIL chamber prototypes.

Table 2: Results of the pitch value from 2-D analysis for the two different BIL chamber prototypes measured: BIL-I, and BIL-R. The values are in micrometres. Results are presented in the MDT reference system.

Multi		$\Delta Z = Z_{measured}$-30000 ↕ ΔY				Interlayer distances - 30000 (Sigma)							
		ΔZ distance & (sigma)		sigma ΔY									
layer		BIL-I	BIL-R	BIL-I	BIL-R	BIL-I	BIL-R	BIL-I	BIL-R	BIL-I	BIL-R	BIL-I	BIL-R
2	3	7.3 (19.7)	95.1 (24.7)	18.6	53.3	-0.7 (19.6)	111.6 (39.7)			-2.8 (18.3)	100.1 (18.0)		
	2	10.4 (26.8)	99.6 (13.2)	22.6	39.1			8.5 (17.9)	137.6 (23.8)			-13.3 (18.4)	126.6 (28.3)
	1	7.0 (18.2)	98.6 (14.8)	22.6	31.0								
1	3	7.8 (22.0)	96.0 (15.1)	23.7	25.6	6.6 (24.5)	123.0 (17.2)			-8.7 (18.6)	111.5 (14.5)		
	2	8.3 (21.2)	97.7 (14.6)	22.4	20.3			-0.7 (19.0)	154.7 (26.3)			-4.2 (20.0)	119.7 (29.8)
	1	7.7 (13.7)	99.2 (15.6)	24.4	36.0								

The results for each individual shift wire position for a complete chamber cross-section are well-represented in a graphical way: we show in Fig. 14 a typical example of a shift map (BIL-I prototype).

As could be expected from the better accuracy obtained in the 2-D analysis, the dispersion (r.m.s.) of the wire pitch (in X) per layer gave better results than those obtained in the 1-D analysis. The preliminary results also confirm the validity of the one-dimensional analysis for the determination of the pitch value. In the 2-D analysis of the four chamber prototypes, the pitch r.m.s. values are (11 ÷ 28) mm in X and (16 ÷ 53) mm in Z (some inside and some outside the design construction value of 20 mm).

However, at the early stage, some results looked strange to chamber constructors: a large shift in the Z position of wires was found for the tubes of multilayers lying at or close to the edges of a chamber prototype. A thorough investigation about possible systematics, perhaps generated by the calibration procedure, is under detailed study in order to disentangle this discrepancy. The first conclusion [19] is the possible existence of systematics in the optical measurement of the calibration ruler. With a view to full systematics control, a new calibration ruler will be made and installed at the bottom, just facing the scintillators: this will eliminate possible systematics in Y and Z.

At this point, it is important to stress that the repeatability of the measurements has been demonstrated within the full range in Z and Y by successive scannings of the BML chamber and by rotating (left, right, and upside down) and remeasuring the BMS prototype in four different positions. The reproducibility of the results, r.m.s. values layer by layer, was excellent and compatible with an accuracy of the tomograph ≤ 10 μm.

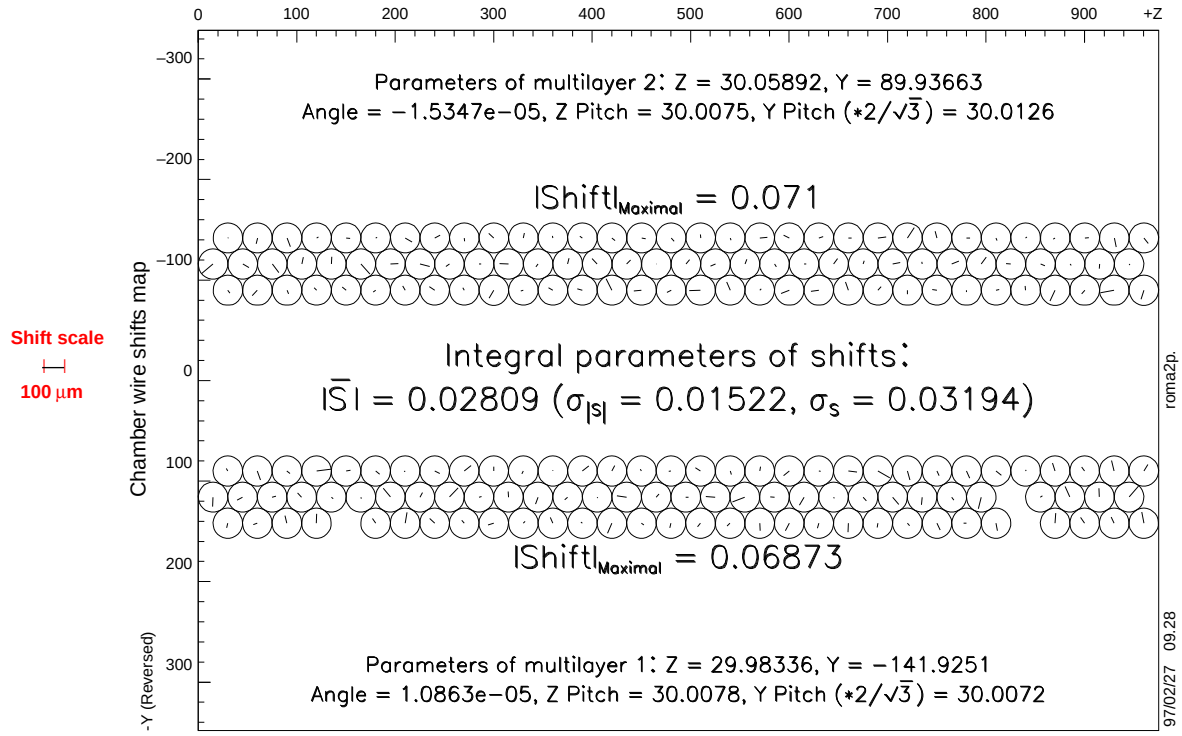

Fig. 14: Reconstructed wire displacement in millimetres in the BIL-I prototype. The lines inside the tubes represent both, the absolute value of the displacement and its direction. Global parameters are calculated: average of absolute shift ($|\bar{S}|$) and r.m.s. value, r.m.s. of the r.m.s. value of the shift projections, and maximum absolute shift value of the two multilayers. Results are presented in the MDT reference system.

5.6 Tomograph upgrading

During the first measurement campaign, we have learned a lot about the tomograph which allows us to proceed to the second phase of the prototype development towards a full X-tomograph quality control robot needed for the future.

A major upgrade [20], aimed at shortening the scanning time and reducing systematic errors, is currently under way. In late 1997, more prototypes will be scanned to assess chamber assembly schemes. From 1998 on, the series production will be validated by X-ray tomography.

The major upgrading concerns the installation of final interferometers with fast VME data acquisition for reducing the scanning duration, the construction and installation of new calibration rulers for improving systematics correction, and our confidence in the results and the automatic displacement and alignment of the chambers under the portico.

It is also foreseen to install a rotating X-ray beam for the measurement of the wire centring and the detection of fiducial wires and hidden tubes.

We also wish to improve the reliability of the system as much as possible.

5.7 Future plans

After the full upgrade, the tomograph will be ready to begin mass non-stop measurements by the end of 1998, when the industrial delivery of MDTs is expected to start.

At present, it is envisaged to spread the industrial fabrication of the MDTs over many sites (≈ 10), in different countries around the world, with different expertise and constraints.

After the upgrading, the X-ray tomograph built at CERN should have a capacity to measure 100 chambers a year (including tomograph maintenance). This should be enough to validate the assembly methods of the series production from every site.

We have to decide the long-term strategy for the assurance quality control early enough in order to leave time to be prepared for the mass industrial delivery of the years 1999 to 2003.

With a single tomograph, less than half the chambers could be measured.

We should also be ready to rescan some chambers at regular intervals, in order to study the long-term stability which is the key to success. Monitoring the space position of the chambers during the experiment would be useless if chambers were to become unstable. Storage, ageing, creeping, transport, temperature constraints, recovery, handling, etc. must be studied continuously.

If we have to measure and control over the years of storage all chambers at CERN before the ATLAS final assembly, it would be necessary to build two fully robotized X-tomographs.

6 CONCLUSION

The X-ray tomograph prototype, combining precise mechanics and the use of interferometers to monitor the space position of X-ray beams, has proved that a 10 μm accuracy measurement of the positioning of the MDT drift tubes is achievable.

It was also demonstrated that the use of a reference grid for a continuous calibration of the X-tomograph was essential for reaching the required accuracy and ensuring full repeatability of the measurements over a long period of time.

The X-tomograph will be a key element for qualifying the MDTs at CERN before the ATLAS muon final assembly. It will also be an essential platform for controlling the chamber stability during the long storage period at CERN before assembly.

It is known from industrial experience that it is always rewarding to invest in quality control and hazardous to avoid it.

Acknowledgements

We would like to thank L. Vertogradov for the excellent pioneering work which he accomplished on the X-ray tomography for the MDT chambers. We are grateful to J. Berbiers and to the members of the ECP/EOS group participating in this X-QC project for their efficient technical assistance throughout the design and construction of the tomograph. We also thank the EST/MF and SU groups for the precise survey of the tomograph and, in particular, C. Boudineau for his competence and enthusiasm in the preparation and installation of the interferometers.

Finally, we address our thanks to the Managements of the ATLAS Collaboration and of the Muon Spectrometer System for their advice and continuous support.

References

[1] ATLAS Experiment on www: http://atlasinfo.cern.ch:80/ATLAS/Welcome.html.

[2] ATLAS Technical proposal, CERN/LHCC/94–43, LHCC/P2, 15 December 1994.

[3] ATLAS muon spectrometer technical design report, CERN/LHCC/97–22, ATLAS TDR 10, 31 May 1997.

[4] ISO 9000-1, Quality management and quality assurance standards—Part 1: Guidelines for selection and use, International Organization for Standardization, 1994, [http://www.iso.ch];
ISO 9000-2, Quality management and quality assurance standards—Part 2: Generic guidelines for the application of ISO 9001, ISO 9002 and ISO 9003, International Organization for Standardization, 1997, [http://www.iso.ch];
ISO 9000-3, Quality management and quality assurance standards—Part 3: Guidelines for the application of ISO 9001 to the development, supply and maintenance of software, International Organization for Standardization, 1991, [http://www.iso.ch];
ISO 9000-4, Quality management and quality assurance standards—Part 4: Guide to dependability programme management, International Organization for Standardization, 1993, [http://www.iso.ch].

[5] ISO 9001, Quality systems—Model for quality assurance in design, development, production, installation and servicing, International Organization for Standardization, 1994, [http://www.iso.ch].

[6] ISO 9002, Quality systems—Model for quality assurance in production, installation and servicing, International Organization for Standardization, 1994, [http://www.iso.ch].

[7] ISO 9003, Quality systems—Model for quality assurance in final inspection and test, International Organization for Standardization, 1994, [http://www.iso.ch].

[8] ISO 9004-1, Quality management and quality system elements—Part 1: Guidelines, International Organization for Standardization, 1994, [http://www.iso.ch];
ISO 9004-2, Quality management and quality system elements—Part 2: Guidelines for services, International Organization for Standardization, 1991, [http://www.iso.ch];

ISO 9004-3, Quality management and quality system elements—Part 3: Guidelines for processed materials, International Organization for Standardization, 1993, [http://www.iso.ch];
ISO 9004-4, Quality management and quality system elements—Part 4: Guidelines for quality improvement, International Organization for Standardization, 1993, [http://www.iso.ch].

[9] Engineering data management—A tool for technical coordination, G. Bachy et al., CERN MT/95–07 (DI).

[10] ATLAS Project, Introduction to the ATLAS quality assurance plan, G. Bachy, Note ATL-CER-QA-001, 22 April 1996.

[11] L. Vertogradov, High precision wire positions measuring in the drift tube package by X-ray scanner (X tomography), ATLAS Internal Note, MUON-041, 11 May 1994.

[12] D. Alexeev et al., XTOMO, a prototype of the X-Ray tomograph for high precision measurements of the MDT muon chambers, ATLAS Internal Note, MUON-142, 24 March, 1997.

[13] D. G. Drakoulakos et al., XTOMO, one-dimensional X-ray scanning of 8-layer MDT prototype using the passive mode, ATLAS Internal Note, MUON-151, 17 April, 1997.

[14] D. G. Drakoulakos et al., XTOMO2, stereo measurements of the MDT muon chambers using a high precision X-ray tomograph, ATLAS Internal Note, MUON-155, April, 1997.

[15] D. G. Drakoulakos, Thesis, to be published in 1997.

[16] F. Lejal et al., On-line conception of the X-tomograph, http://wwwcn.cern.ch/~lejal/LINKS/internalNote.ps.

[17] E. Gschwendtner, Diploma thesis, to be published summer 1997.

[18] X-TOMO Web reference addresses: http://wwwcn.cern.ch/~sedykh/X-tomo.

[19] Y. Sedykh et al., Stereo measurements of large full scale MDT prototypes, to be issued summer 1997 as CERN-ATLAS, MUON-NO-175.

[20] J. Berbiers et al., X-ray tomograph prototype for MDT quality control, status of the X-QC project, past and future, CERN-ATLAS, MUON-NO-174,14 July 1997.

FrameMaker has detected one or more PostScript errors in this document.
(David Stungo)
Please check your output.